Supplementary Information

Lithium - Activated SnS - Graphene Alternating Nanolayers Enable Dendrite-Free Cycling of Thin Sodium Metal Anodes in Carbonate Electrolyte

Table S1. A broad performance comparison of A-SnS-G@Na || A-SnS-G@Na symmetric cells versus state-of-the-art symmetric Na||Na architectures from literature. [1-9]

A = accumulated capacity = capacity per cycle x cycle number, in units of mAh cm^{-2}

F = foil capacity = thickness of foil x ρ_{Na} x theoretical capacity.

For 100 μm foil: F = 100 x 10^{-4} cm x 0.97 g cm^{-3} x 1165 mAh g^{-1} = 11 mAh cm^{-2}

A/F ratio= accumulated capacity / foil capacity

	Symmetric Na-Na Cells		
Architecture, Electrolyte, Foil Thickness	**Current density (capacity)**	**Accumulated capacity (number of cycles)**	**A/F ratio**
A-SnS-G membrane (1M $NaClO_4$ EC/DEC/FEC) (100 μm Na)	**4 mA cm^{-2} (2 mAh cm^{-2})**	**1000 mAh cm^{-2} (500 cycles)**	**90.9**
ALD-Al_2O_3 protection (1M $NaClO_4$ EC/DEC) (unspecified thickness)[1]	0.5 mA cm^{-2} (1 mAh cm^{-2})	30 mAh cm^{-2} (30 cycles)	NA
Hybrid electrolyte coated Na (PVDF-HFP polymer gel) (unspecified thickness)[2]	2 mA cm^{-2} (1 mAh cm^{-2})	100 mAh cm^{-2} (100 cycles)	NA
CVD graphene protection (1M $NaPF_6$ in EC/DEC) (indeterminate thickness)[3]	2 mA cm^{-2} (3 mAh/cm^{-2})	300 mAh cm^{-2} (100 cycles)	NA

Nanoparticle interface (0.01M NaTFSI+1M $NaSO_3CF_3$ in diglyme) (1000 µm Na)[4]	2 mA cm^{-2} (2 mAh/cm^{-2})	1200 mAh cm^{-2} (600 cycles)	~10.7
Carbon felt hosted Na (1M $NaClO_4$ EC/PC) 500 µm Na[5]	5 mA cm^{-2} (2 mAh cm^{-2})	250 mAh cm^{-2} (125 cycles)	~4.5
Channeled carbons host (1M $NaClO_4$ EC/DEC) (Na>500 µm)[6]	1 mA cm^{-2} (1 mAh cm^{-2})	500 mAh cm^{-2} (500 cycle)	~8.9
N,S doped C-nanotube host (1M sodium triflate in diglyme) (~200 µm Na)[7]	1 mA cm^{-2} (1 mAh cm^{-2})	250 mAh cm^{-2} (250 cycles)	~11.1
Sn interlayer protection (Sn coated solid-state electrolyte) (300 µm Na)[8]	0.5 mA cm^{-2} (0.5 mAh cm^{-2})	250 mAh cm^{-2} (500 cycles)	~7.4
Single Zn on nitrogen doped carbon cloth (1M $NaClO_4$ EC/DMC/FEC) (unspecified thickness)[9]	1 mA cm^{-2} (1 mAh cm^{-2})	150 mAh cm^{-2} (150 cycles)	~37.5

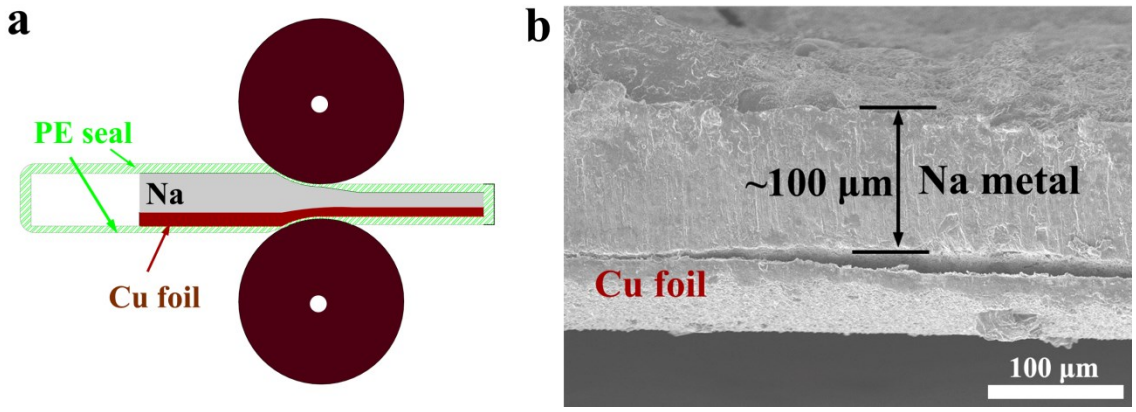

Figure S1. (a) Schematic illustration of the PE seal protected rolling process to fabricate thin Na metal foils. **(b)** SEM image of the rolled foil, highlighting its uniform thickness.

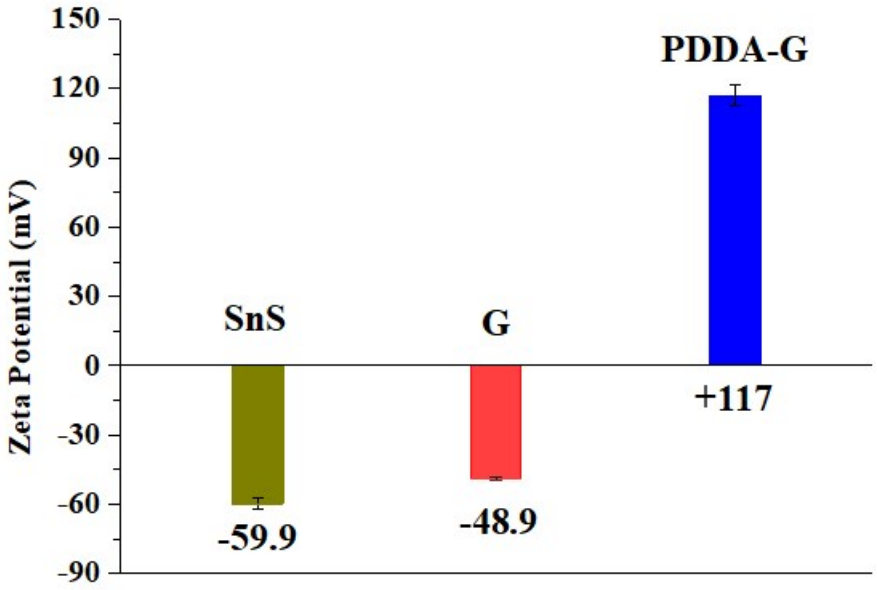

Figure S2. Zeta potential of as-synthesized SnS nanosheets (SnS), graphene (G) and PDDA modified graphene (PDDA-G).

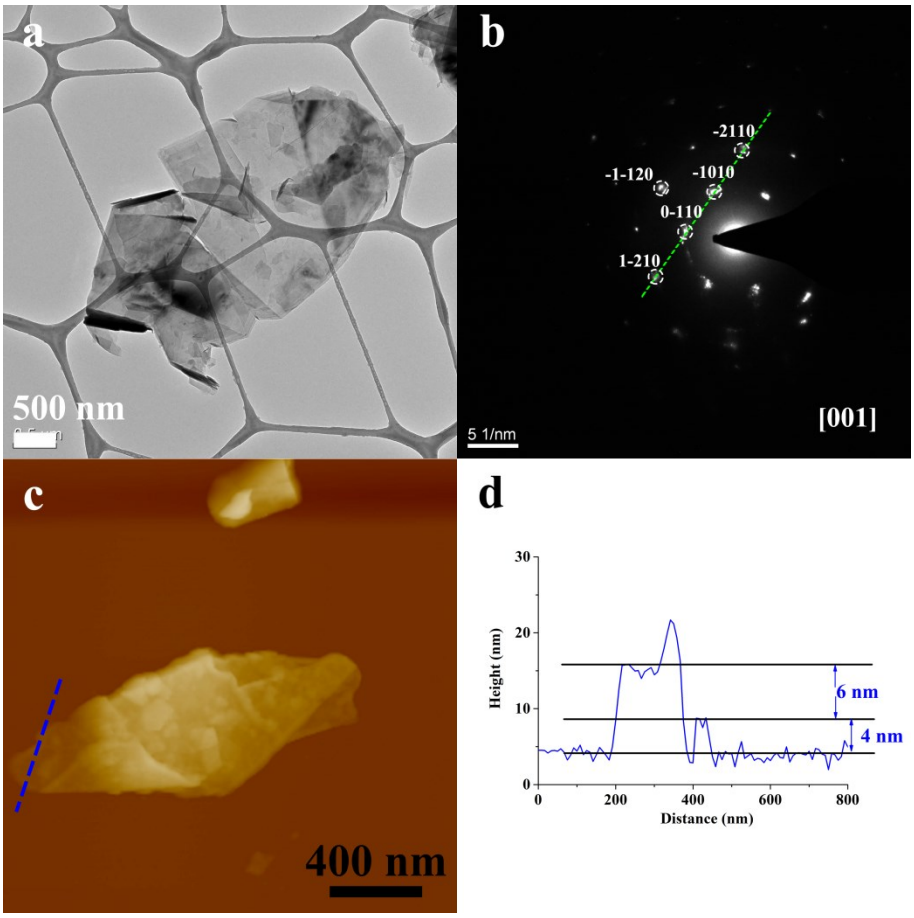

Figure S3. (a) - (b) Bright field TEM image and associated [001] Zone Axis SAED of the as-synthesized graphene. **(c) - (d)** AFM image the corresponding height profile of the as-synthesized graphene deposited onto a mica substrate.

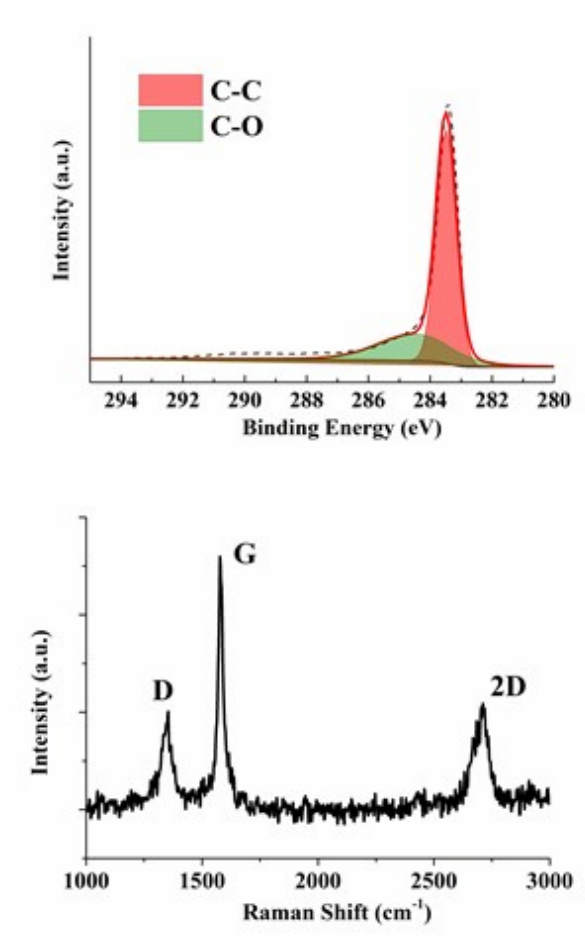

Figure S4. XPS C 1s spectra (top) and the Raman spectra of the as-synthesized graphene layers.

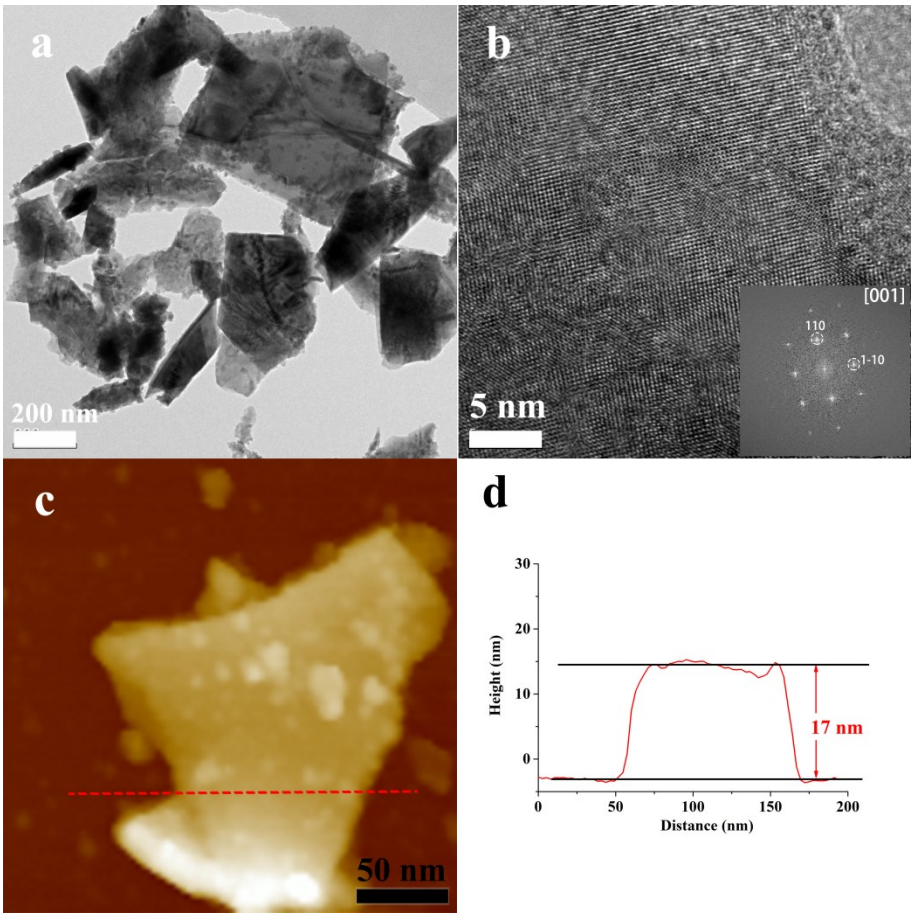

Figure S5. (a) Bright field TEM image of as-synthesized SnS nanosheets. **(b)** HRTEM image in the [001] zone axis highlighting the highly ordered SnS structure. Inset shows the corresponding FFT pattern. **(c)** and **(d)** AFM image and the associated height map of a single SnS nanosheet on a mica substrate.

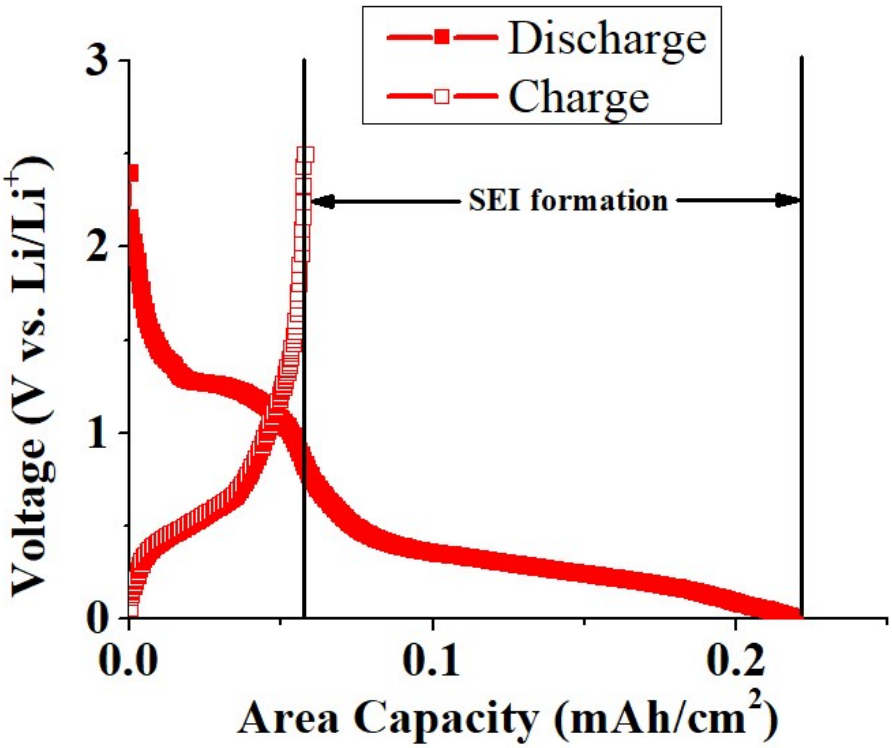

Figure S6. The Li activation process of SnS-G, with the irreversible capacity largely corresponding to the formation of a Li-based SEI.

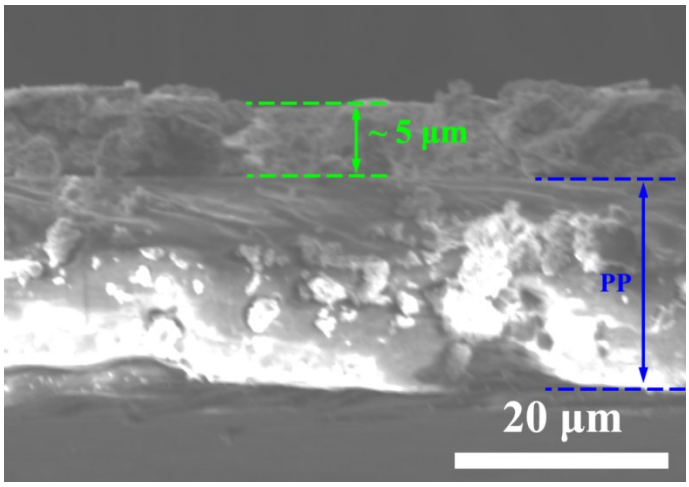

Figure S7. Cross sectional SEM image of the as-synthesized SnS-G film deposited on top of the PP separator.

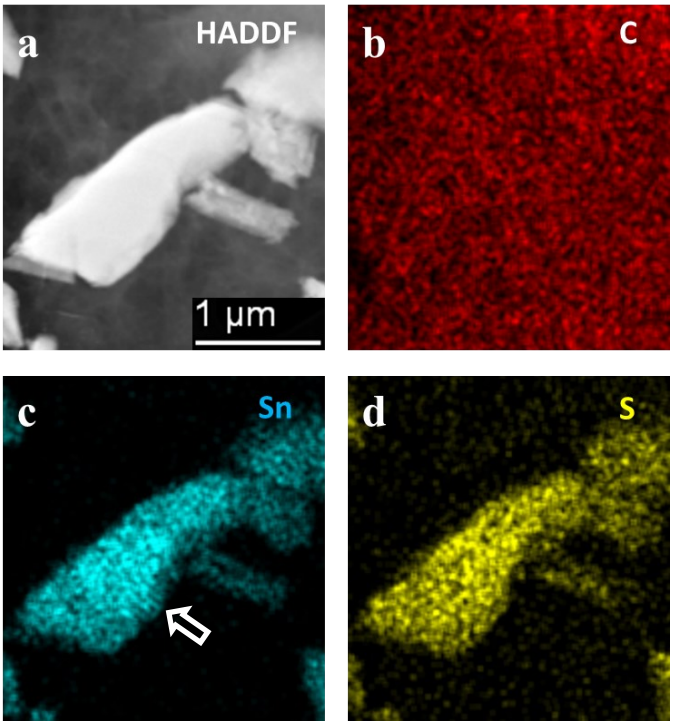

Figure S8. HADDF-TEM images (a) of as-synthesized SnS-G composite and (b)-(d) EDS elemental mapping of C, Sn and S.

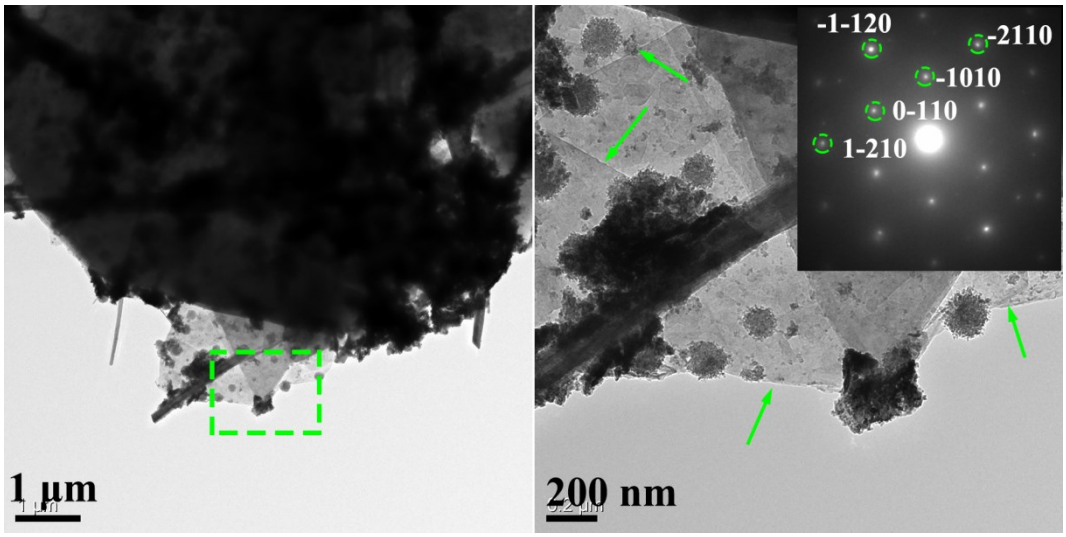

Figure S9. TEM and associated SAED analysis of A-SnS-G. The intact structure of the graphene is evidenced by the TEM images showing the characteristic sheet-like morphology, and the associated [0001] zone axis diffraction pattern displaying hexagonal symmetry. The Sn and S phases in the delithiated state are diffraction amorphous. Arrows point to the graphene layer edges.

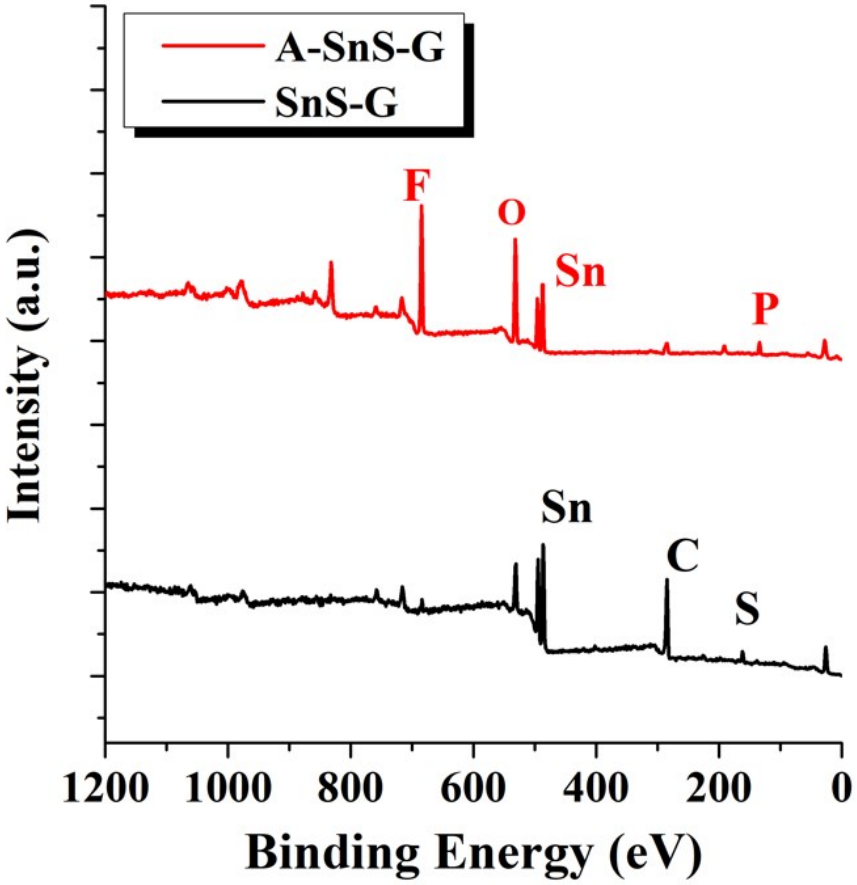

Figure S10. XPS overview spectra of SnS-G and A-SnS-G

Table S2. Four probe conductivities of as-prepared membrane (SnS-G@PP) and Li activated membrane (A-SnS-G@PP), in each case 10 separate tests were carried out to calculate an average value.

Sample	Conductivity
A-SnS-G@PP	≈0.001 $S \cdot cm^{-1}$ (±15%)
SnS-G@PP	0.22 $S \cdot cm^{-1}$ (±7%)

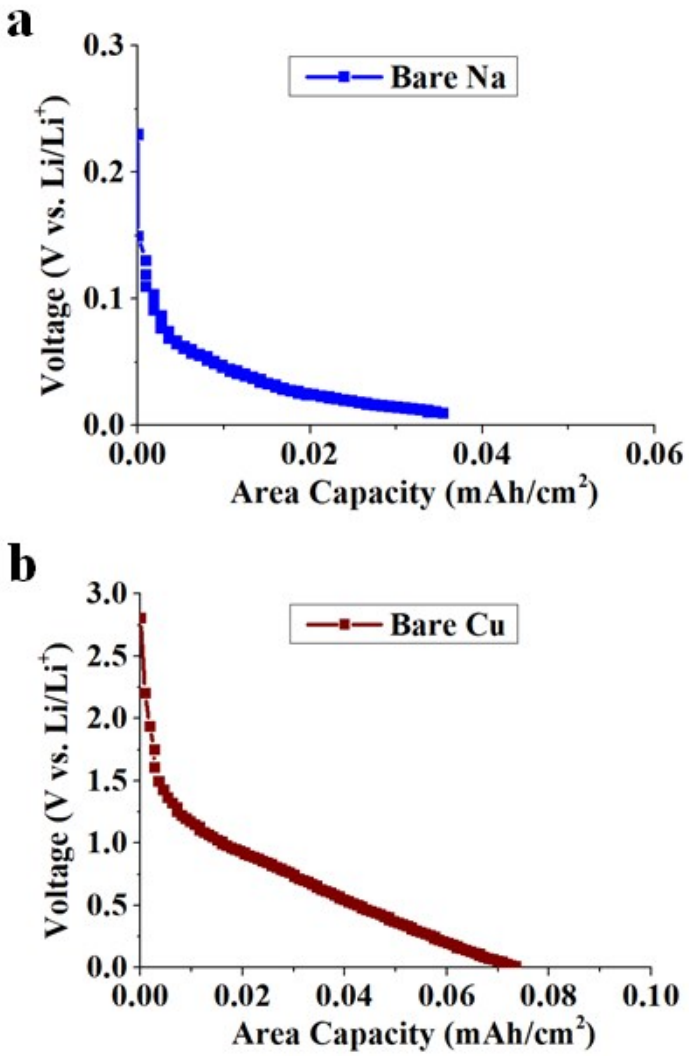

Figure S11. Lithium - activation process of bare Na foil (a) and Cu foil (b). The lower voltage cutoff is 0.01 V vs. Li/Li^+, above the equilibrium plating voltage of Li. Therefore, all irreversible capacity corresponds to the decomposition of Li-electrolyte that leads to the formation of a Li-based SEI.

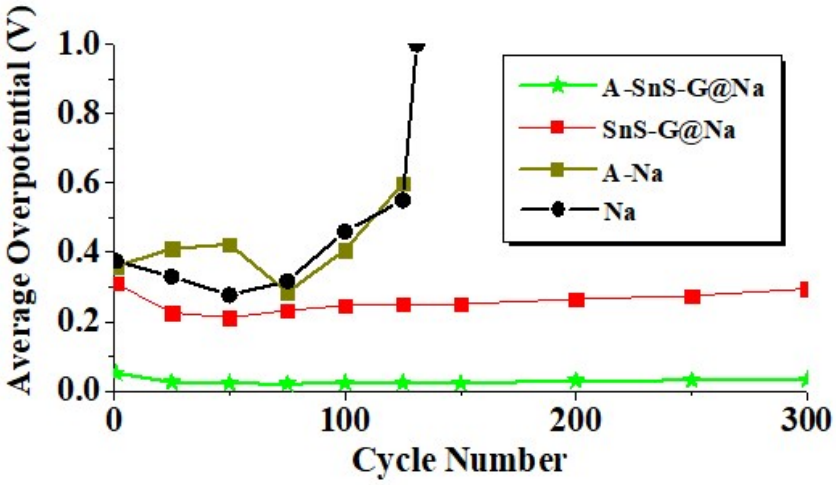

Figure S12. Average overpotential of Na-Na symmetric cells cycling at current density of 1mA cm^{-2}.

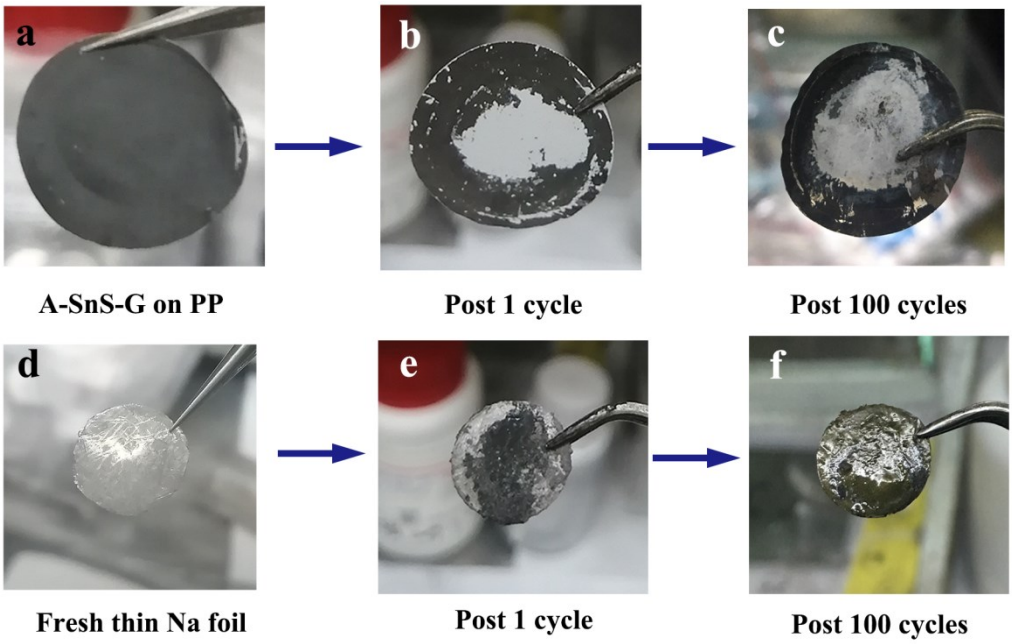

Figure S13. Light optical images illustrating the cycling-induced in-situ transfer process of A-SnS-G layer from the PP separator to the thin Na metal surface. (a) A-SnS-G layer initially deposited on the PP; (b) Post 1 cycle separator with part of A-SnS-G layer missing; (c) Post 100 cycles separator with more of A-SnS-G layer missing; (d) - (f) Images of the associated Na metal anodes.

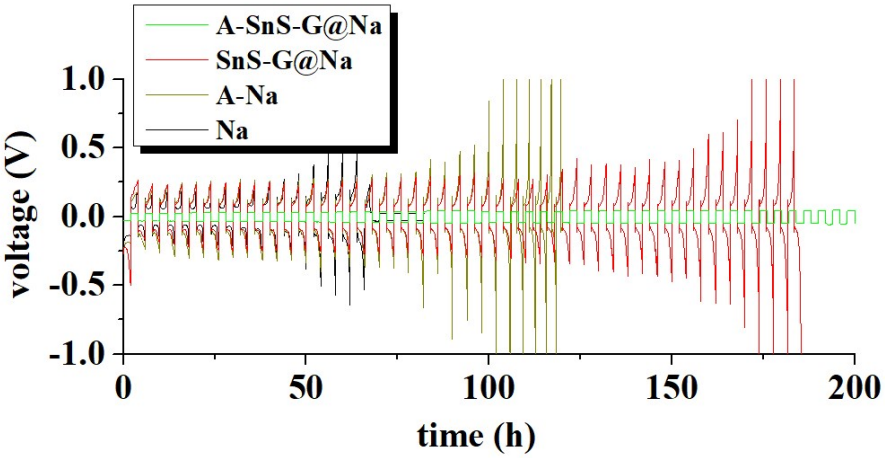

Figure S14. Voltage - time profiles of symmetric cells tested at 1 mA cm^{-2} with 2 hours plating time per cycle.

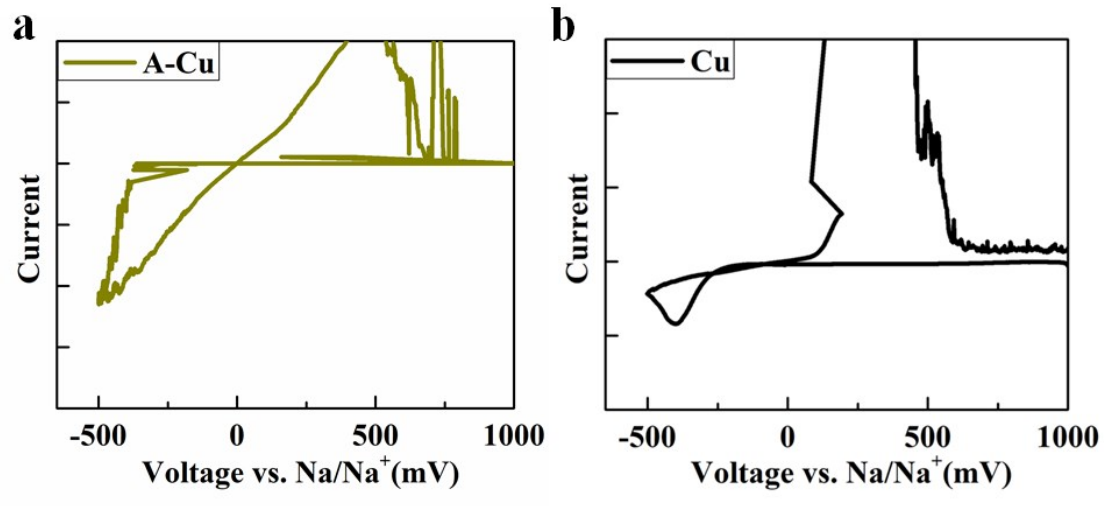

Figure S15. CV curves of Na metal plating-stripping onto (a) A-Cu and (b) bare Cu.

References

1. W. Luo, C.-F. Lin, O. Zhao, M. Noked, Y. Zhang, G. W. Rubloff and L. Hu, *Adv. Energy Mater.*, 2017, **7**, 1601526.
2. D. Lei, Y.-B. He, H. Huang, Y. Yuan, G. Zhong, Q. Zhao, X. Hao, D. Zhang, C. Lai, S. Zhang, J. Ma, Y. Wei, Q. Yu, W. Lv, Y. Yu, B. Li, Q.-H. Yang, Y. Yang, J. Lu and F. Kang, *Nat. Commun.*, 2019, **10**, 4244.
3. H. Wang, C. Wang, E. Matios and W. Li, *Nano Lett.*, 2017, **17**, 6808-6815.
4. S. Tang, Y.-Y. Zhang, X.-G. Zhang, J.-T. Li, X.-Y. Wang, J.-W. Yan, D.-Y. Wu, M.-S. Zheng, Q.-F. Dong and B.-W. Mao, *Adv. Mater.*, 2019, **31**, 1807495.
5. S. S. Chi, X. G. Qi, Y. S. Hu and L. Z. Fan, *Adv. Energy Mater.*, 2018, **8**, 1702764.
6. W. Luo, Y. Zhang, S. Xu, J. Dai, E. Hitz, Y. Li, C. Yang, C. Chen, B. Liu and L. Hu, *Nano Lett.*, 2017, **17**, 3792-3797.
7. B. Sun, P. Li, J. Zhang, D. Wang, P. Munroe, C. Wang, P. H. L. Notten and G. Wang, *Adv. Mater.*, 2018, **30**, 1801334.
8. X. Chi, F. Hao, J. Zhang, X. Wu, Y. Zhang, S. Gheytani, Z. Wen and Y. Yao, *Nano Energy*, 2019, **62**, 718-724.
9. T. Yang, T. Qian, Y. Sun, J. Zhong, F. Rosei and C. Yan, *Nano Lett.*, 2019.